Solitons in nonlinear fiber couplers with two orthogonal polarizations

T. I. Lakoba
Department of Mathematics and Computer Science, Clarkson University, Potsdam, New York 13699-5817

D. J. Kaup
Department of Mathematics and Computer Science and Department of Physics, Clarkson University, Potsdam, New York 13699-5815

B. A. Malomed
Department of Interdisciplinary Studies, Faculty of Engineering, Tel Aviv University, Tel Aviv 69978, Israel
(Received 11 October 1996)

We consider a model of two coupled nonlinear optical fibers with two polarizations in each fiber. This study only considers the two cases when the polarization of the light in each fiber is either linear or circular. We use the variational method to find families of stationary solitary waves (solitons) of this model. In particular, we demonstrate that the variational method can be used in a universal fashion to find certain types of bifurcations of the stationary solutions. All the families of solitons that we find can be classified in three groups: (i) core-symmetric solitons that have equal energies in each core, (ii) core-asymmetric solitons that for large values of the energy have most of the energy concentrated in one core, and (iii) core-asymmetric solitons for which the ratio of the energies in the two cores remains finite when the total energy of the soliton becomes very large. The first two groups of solitons have direct analogs with solitons of the nonlinear fiber coupler that has only one polarization in each core. We also briefly discuss the stability properties of the various solitons found. [S1063-651X(97)07805-7]

PACS number(s): 03.40.Kf, 42.65.Tg, 42.81.Gs

I. INTRODUCTION

Solitons and other nonlinear states in coupled optical fibers [nonlinear directional couplers (NLDCs)] have been extensively studied theoretically over the past several years; see, e.g., Refs. [1–9]. Besides being of interest in their own right, such solitons may find applications in future communication systems as information carriers in all-optical switching devices [9]. Past works have only considered models in which each core of the NLDC was monomode. In reality however, it is necessary to take into account the polarization of light. If one allows two polarizations in the coupled cores, this will render the system's dynamics richer than it would be in the case of monomode cores, and will open the way to predict new types of solitons, as well as their bifurcations. This is the general objective of the present work.

We consider a model based on the equations

$$\begin{aligned} iu_{1,z}+\tfrac{1}{2}u_{1,\tau\tau}+u_1(|u_1|^2+\beta|v_1|^2)+\kappa u_2=0,\\ iv_{1,z}+\tfrac{1}{2}v_{1,\tau\tau}+v_1(|v_1|^2+\beta|u_1|^2)+\kappa v_2=0,\\ iu_{2,z}+\tfrac{1}{2}u_{2,\tau\tau}+u_2(|u_2|^2+\beta|v_2|^2)+\kappa u_1=0,\\ iv_{2,z}+\tfrac{1}{2}v_{2,\tau\tau}+v_2(|v_2|^2+\beta|u_2|^2)+\kappa v_1=0, \end{aligned} \tag{1.1}$$

which describes pulse propagation in two adjacent fiber cores, with two orthogonal polarizations existing in each core. In Eqs. (1.1) we have used the standard nondimensionalized variables $u_{1,2}$ and $v_{1,2}$ for the envelopes of the electric field in the pulse, and z and τ for the distance along the fiber and for the retarded time, respectively (cf., e.g., [10,11,6]). Each polarization component in a core is coupled linearly to the parallel polarization component in the other core, while inside the same core, the orthogonal polarization components are coupled nonlinearly. We will consider the cases when $\beta=\frac{2}{3}$ and $\beta=2$, which correspond, respectively, to propagation of linearly and circularly polarized light inside each core (cf. [12]). Any values of β between $\frac{2}{3}$ and 2 will correspond to elliptically polarized eigenmodes (cf. [11,12]); however, we will restrict ourselves to considering only these two cases. Let us note that the case $\beta=2$ pertains not only to two circularly polarized modes but also to two parallel, linearly polarized modes with distinct carrier wavelengths. The linear coupling constant κ can always be scaled ([14]) to an arbitrary (nonzero) value. Thus, in what follows, we will set

$$\kappa=1.$$

We will refer to Eqs. (1.1) as the ''dual core, dual polarization'' (DCDP) model.

One of the main assumptions made in the derivation of the DCDP equations is that there is a large phase birefringence in each core, so that the birefringence beat length between the orthogonal polarizations is much shorter than the nonlinear, dispersion, and coupling lengths, with the latter three lengths being of the same order of magnitude. Given the large birefringence of the cores, one can then discard certain rapidly oscillating terms (cf. [11,12]) and, after a simple phase transformation, obtain Eqs. (1.1). The other two assumptions made in the derivation of Eq. (1.1) are that (i) the propagation constants of the parallel polarizations are equal, (ii) as are the linear coupling constants for the vertical and horizontal polarizations.

As mentioned above, the DCDP generalizes the celebrated equations of the NLDC that have only one polariza-

tion in each core (for a review see, e.g., [7], and references therein). (The latter model will be referred to simply as NLDC throughout the text.) On the other hand, in the limit when the linear coupling constant between the parallel polarizations vanishes and one obtains two uncoupled cores, the DCDP reduces to another well-studied case, that of two orthogonally polarized pulses propagating in the same core. (In such a case, the pulses in the orthogonal polarizations are said to form a *vector soliton*.) Thus it is natural to develop our analysis, as well as to present the results, for the DCDP proceeding from the results already known for the two aforementioned basic models. The most important piece of information pertaining to these models is the form of their stationary, solitonlike solutions; for brevity, we will call such solutions simply ''solitons'' without implying that Eqs. (1.1) are integrable by the inverse scattering transform. The reason why we restrict our attention only to solitons is that even though there are other types of stationary solutions, whose intensity profile has more than one maximum, they have always been found to be structurally unstable (see, e.g., [4,13,14]), and thus they do not seem to be important in the evolution of an arbitrary initial pulse.

In this paper, we study the problem of the existence of soliton solutions of the DCDP. To this end, we employ the variational method (see Sec. III below), which yields six nonlinear algebraic equations for the amplitudes and widths of the soliton's components. Those equations can be solved, in general, only numerically; however, certain important information about the solutions can be obtained either analytically or by numerically solving only two (instead of six) equations. We will also briefly report on the main results about the stability of the solitons found, with a more detailed exposition of the stability analysis being given elsewhere ([15]).

The rest of the paper is organized as follows. In Sec. II we review the results for the soliton solutions of the two basic models: the NLDC and the single core with two orthogonal polarizations. In Sec. III, we formulate the variational method for the DCDP (1.1), derive six algebraic equations for the amplitudes and widths of the soliton's four components ($u_{1,2}$ and $v_{1,2}$), and then present some simple solutions to those equations in special cases. In Sec. IV we find the boundaries of the regions of existence of various types of solitons of the DCDP. Some of those boundaries can be determined quite simply analytically, while the others can be determined by solving numerically two nonlinear algebraic equations, obtained from the full set of six equations. Among the latter group of the boundaries, there are bifurcation curves that correspond to a *pitchfork bifurcation* that occurs to a core-symmetric soliton [see the definition after Eqs. (3.13)] thereby giving rise to a core-asymmetric one. Let us note that although the method we used to find these bifurcation curves is quite simple, we are not aware of any earlier works where such a method has been used for the same purpose. In Sec. V, we present and discuss the results of the numerical solution of the full set of equations, Eqs. (3.3). In Sec. VI, we summarize the results of this work and also briefly describe the stability of the various types of solitons in the limit of large energy. In general, in that limit, only solitons that are four-component analogs of the asymmetric soliton of the NLDC are stable. However, as it has been found in [15], there are two other types of solitons of the DCDP. Solitons of one of these types, although being unstable, have a much slower instability growth rate than that of all the other unstable solitons. The stability of the second type of solitons has not and could not be established within the framework of first-order calculations. Thus even if the latter type of solitons may be found to be unstable in future studies, its instability growth rate will still be quite low, thus it may be useful as an intermediate state, and even important in the evolution of an arbitrary initial pulse.

II. REVIEW OF THE TWO BASIC MODELS

We start with a review of the NLDC model. It is described (see, e.g., [7,6]) by two linearly coupled nonlinear Schrödinger (NLS) type equations

$$\begin{aligned} iu_{1,z}+\tfrac{1}{2}u_{1,\tau\tau}+u_1|u_1|^2+u_2=0,\\ iu_{2,z}+\tfrac{1}{2}u_{2,\tau\tau}+u_2|u_2|^2+u_1=0, \end{aligned} \tag{2.1}$$

in which we have set the linear coupling constant between the cores equal to unity. Soliton solutions of Eqs. (2.1) can be found in the form

$$u_n(z,\tau)=e^{ipz}u_n(\tau), \quad n=1,2, \tag{2.2}$$

where $p=\text{const}$ and $u_n(\tau)$ are real valued.

Equations (2.1) possess symmetric [with $u_1(\tau)=u_2(\tau)$] and antisymmetric [with $u_1(\tau)=-u_2(\tau)$] solutions, which exist for $p\geqslant 1$ and $p\geqslant -1$, respectively:

$$\begin{aligned} u_1^{(s)}(\tau)=u_2^{(s)}(\tau)=\sqrt{2(p-1)}\,\mathrm{sech}[\sqrt{2(p-1)}\,\tau],\\ u_1^{(an)}(\tau)=-u_2^{(an)}(\tau)=\sqrt{2(p+1)}\,\mathrm{sech}[\sqrt{2(p+1)}\,\tau]. \end{aligned} \tag{2.3}$$

In [3], it was shown that in addition to these two types of solutions, for $p\geqslant\frac{5}{3}$, there exists an asymmetric solution with $u_1(\tau)u_2(\tau)>0$ and $u_1(\tau)\neq u_2(\tau)$. An exact analytical form of the asymmetric solution is not known; however, an approximate expression can be found with the variational method (see Sec. III). It should be noted that the asymmetry between the components of the asymmetric solution is absent at the point of the *pitchfork bifurcation*, $p=\frac{5}{3}$. Asymptotically, as $p\to\infty$, $u_1(\tau)/u_2(\tau)=O(p)$.

In [4], a numerical study of stability of these three types of stationary solutions was undertaken, and its results can be summarized as follows.

(i) The antisymmetric solution is unstable with respect to small perturbations of its shape for $p\geqslant -0.6$, [this value was read off of Fig. 1(a) in [4]] i.e., in almost the entire region of its existence.

(ii) The symmetric solution is stable for $p\leqslant\frac{5}{3}$, i.e., up to the bifurcation point, where it loses stability and remains unstable for all larger values of p.

(iii) The asymmetric solution is unstable in a tiny region $\frac{5}{3}\leqslant p\leqslant 1.85$, and is stable for $p\geqslant 1.85$. The existence of that small region of instability indicates that the bifurcation at $p=\frac{5}{3}$ is subcritical. That is, for $\frac{5}{3}<p<1.85$, the slope $dE/dp<0$, where the soliton's energy E is defined by

$$E=\int_{-\infty}^{\infty} d\tau(|u_1|^2+|u_2|^2).$$

The subcritical nature of the bifurcation was first discovered numerically in [4], and recently it was shown [8] that the variational method can also grasp this feature. In the present work, however, we will restrict our attention to only finding the location of the corresponding bifurcation points for Eqs. (1.1), without resolving the question of whether those bifurcations are subcritical or not.

The second basic model is a single core with two orthogonal, nonlinearly coupled polarizations. It is described by the following equations:

$$\begin{aligned} iu_z+\tfrac{1}{2}u_{\tau\tau}+u(|u|^2+\beta|v|^2)=0,\\ iv_z+\tfrac{1}{2}v_{\tau\tau}+v(|v|^2+\beta|u|^2)=0, \end{aligned} \tag{2.4}$$

which were first derived in [11]. The values of the nonlinear cross-coupling coefficient, $\beta=\frac{2}{3}$ and $\beta=2$, correspond, respectively, to linearly and circularly polarized eigenmodes in the fiber. We will refer to Eqs. (2.4) as to the ''vector NLS'' (VNLS) equations.

Stationary solutions of Eqs. (2.4) can be found in the form

$$u(z,\tau)=u(\tau)e^{ipz}, \quad v(z,\tau)=v(\tau)e^{iqz}, \tag{2.5}$$

with $u(\tau)$ and $v(\tau)$ being real. We will refer to the solution (2.5) as to a ''vector soliton.'' In [16,17], it was shown that the vector solitons that have both u and v components nonzero exist in a domain of the (p,q) plane located between the straight lines:

$$q_{cr}^{\pm}=\left(\frac{\sqrt{1+8\beta}-1}{2}\right)^{\pm 2}p. \tag{2.6}$$

Outside the above domain, as well as at the boundaries, there are only solutions with either a 0° or a 90° angle of polarization:

$$\begin{aligned} &q=q_{cr}^{+}: \quad u_{00}(\tau)=\sqrt{2p}\,\mathrm{sech}\sqrt{2p}\,\tau, \quad v(\tau)=0,\\ &q=q_{cr}^{-}: \quad u(\tau)=0, \quad v_{00}(\tau)=\sqrt{2q}\,\mathrm{sech}\sqrt{2q}\,\tau. \end{aligned} \tag{2.7}$$

When $p=q$, a solution of the VNLS is a composite vector soliton with a 45° angle of polarization:

$$p=q: \quad |u(\tau)|=|v(\tau)|=\sqrt{2p/(1+\beta)}\,\mathrm{sech}\sqrt{2p}\,\tau \tag{2.8}$$

(the relative sign of u and v is unimportant). For $q_{cr}^{-}<q<q_{cr}^{+}$ and $p\neq q$, an analytical form for the vector soliton, to be denoted as (u_0,v_0), is not known; however, $u_0(\tau)$ and $v_0(\tau)$ can be found numerically; see, e.g., [17]. Lastly, all the vector solitons of the VNLS were found to be stable, and they were shown to have no bifurcations [13].

III. VARIATIONAL METHOD AND ITS SIMPLEST SOLUTIONS

To find the stationary soliton solutions of Eqs. (1.1), we employ the variational method. To this end, we take a Gaussian ansatz for the functions $u_{1,2}$ and $v_{1,2}$:

$$\begin{aligned} u_{1,2}(z,\tau)&=A_{1,2}e^{ipz}e^{-a^2\tau^2/2},\\ v_{1,2}(z,\tau)&=B_{1,2}e^{iqz}e^{-b^2\tau^2/2}. \end{aligned} \tag{3.1}$$

It is known that a Gaussian profile is able to approximate the exact hyperbolic secant soliton of a single NLS equation [18], and also solitons of linearly coupled NLS-type equations [19], quite well. Moreover, as has already been mentioned, the variational method yields rather accurate results, even in the vicinity of the bifurcation that occurs to the symmetric soliton in the NLDC model [8]. Thus, we expect that it will also be able to sufficiently closely approximate the solitons of the DCDP and their bifurcations.

Let us note that the widths of the soliton's components, which are linearly coupled to each other, are taken to be equal, the reason being that earlier numerical results [3,5,19] for linearly coupled NLS-type equations suggested that the widths of the linearly coupled components do not significantly differ. On the other hand, the widths of the orthogonal components, which are only coupled nonlinearly, must be allowed to be different; otherwise, for example, one would not be able to satisfactorily match the exact result (2.6) with its variational approximation [cf. Eq. (4.3) below].

Now, one inserts ansatz (3.1) into the Lagrangian density

$$\begin{aligned} \mathcal{L}=&\frac{i}{2}\sum_{n=1,2}[(u_n^*u_{n,z}-\text{c.c.})+(v_n^*v_{n,z}-\text{c.c.})]\\ &+\sum_{n=1,2}\left[-\frac{1}{2}(|u_{n,\tau}|^2+|v_{n,\tau}|^2)+\tfrac{1}{4}(|u_n|^4+|v_n|^4)\right.\\ &\left.+\frac{\beta}{2}|u_n|^2|v_n|^2\right]+(u_1^*u_2+u_2^*u_1)+(v_1^*v_2+v_2^*v_1) \end{aligned}$$

of Eqs. (1.1) and then integrates the result over τ to obtain the averaged Lagrangian

$$\begin{aligned} \frac{1}{\sqrt{\pi}}\langle\mathcal{L}\rangle=&-\sum_{n=1,2}\left[\frac{1}{8}(A_n^2a+B_n^2b)+\frac{1}{2}\left(A_n^2\frac{p}{a}+B_n^2\frac{q}{b}\right)\right]\\ &+\sum_{n=1,2}\left[\frac{1}{4\sqrt{2}}\left(A_n^4\frac{1}{a}+B_n^4\frac{1}{b}\right)+\frac{\beta}{2}\frac{A_n^2B_n^2}{\sqrt{a^2+b^2}}\right]\\ &+\frac{1}{a}A_1A_2+\frac{1}{b}B_1B_2. \end{aligned} \tag{3.2}$$

Since we are looking for stationary solutions, we set

$$\frac{d}{dz}A_1(z)=\cdots=\frac{d}{dz}b(z)=0.$$

Then the Euler-Lagrange equations, derived from Eq. (3.2), yield the following system of nonlinear algebraic equations for the amplitudes and the widths:

$$\frac{a^2}{4}+p-\frac{A_1^2}{\sqrt{2}}-\beta\frac{B_1^2a}{\sqrt{a^2+b^2}}-\frac{A_2}{A_1}=0, \tag{3.3a}$$

$$\frac{a^2}{4}+p-\frac{A_2^2}{\sqrt{2}}-\beta\frac{B_2^2a}{\sqrt{a^2+b^2}}-\frac{A_1}{A_2}=0, \tag{3.3b}$$

$$\frac{b^2}{4}+q-\frac{B_1^2}{\sqrt{2}}-\beta\frac{A_1^2 b}{\sqrt{a^2+b^2}}-\frac{B_2}{B_1}=0, \tag{3.3c}$$

$$\frac{b^2}{4}+q-\frac{B_2^2}{\sqrt{2}}-\beta\frac{A_2^2 b}{\sqrt{a^2+b^2}}-\frac{B_1}{B_2}=0, \tag{3.3d}$$

$$\left(\frac{a^2}{8}-\frac{p}{2}\right)(A_1^2+A_2^2)+\frac{1}{4\sqrt{2}}(A_1^4+A_2^4)+\frac{\beta}{2}\frac{A_1^2B_1^2+A_2^2B_2^2}{\sqrt{a^2+b^2}}a^3 + A_1A_2=0, \tag{3.3e}$$

while we find it convenient for future use, to write the next equation in the form

$$\left(\frac{b^2}{8}-\frac{q}{2}\right)\left(\frac{B_1}{B_2}+\frac{B_2}{B_1}\right)+\frac{1}{4\sqrt{2}}\left(B_1^2\frac{B_1}{B_2}+B_2^2\frac{B_2}{B_1}\right) + \frac{\beta b^3}{2(\sqrt{a^2+b^2})^3}\left(A_1^2\frac{B_1}{B_2}+A_2^2\frac{B_2}{B_1}\right)+1=0. \tag{3.3f}$$

In the above system of equations, the propagation constants p and q play the role of control parameters.

There are two special cases for which analytical solutions of Eqs. (3.3) are known. The first such case corresponds to the reduction of the DCDP to the NLDC basic model. In this case, set, say, $B_1=B_2=0$, and then Eqs. (3.3a), (3.3b), and (3.3e) yield

$$\frac{a^2}{4}+p-\frac{A_1^2}{\sqrt{2}}-\frac{A_2}{A_1}=0, \tag{3.4a}$$

$$\frac{a^2}{4}+p-\frac{A_2^2}{\sqrt{2}}-\frac{A_1}{A_2}=0, \tag{3.4b}$$

$$\left(\frac{a^2}{8}-\frac{p}{2}\right)(A_1^2+A_2^2)+\frac{1}{4\sqrt{2}}(A_1^4+A_2^4)+A_1A_2=0. \tag{3.4c}$$

By substracting Eq. (3.4a) from Eq. (3.4b), one obtains that either

$$A_1^2=A_2^2 \tag{3.5a}$$

or

$$A_1A_2=\sqrt{2}. \tag{3.5b}$$

Thus we have two subcases. Proceeding with the subcase (3.5a), which obviously corresponds to the symmetric or antisymmetric solitons (2.3) of the NLDC, one obtains from Eqs. (3.4a) and (3.4c)

$$a^2=\tfrac{4}{3}(p-\mu),\quad A_1=\mu A_2=\left(\frac{4\sqrt{2}}{3}(p-\mu)\right)^{1/2},\quad \mu=\pm 1. \tag{3.6}$$

Next, the subcase (3.5b) corresponds to the asymmetric soliton of the NLDC. Although, as was mentioned in Sec. II, an exact analytical form of this solution is not known, one can still solve Eqs. (3.4) and thus find its approximate form. To this end, we denote

$$Z\equiv A_1^2+A_2^2 \tag{3.7}$$

and then add Eqs. (3.4a) and (3.4b) to obtain

$$\frac{a^2}{2}=Z\sqrt{2}-2p, \tag{3.8}$$

where we have used the relation (3.5b). Substituting now Eq. (3.4c) into Eq. (3.8) and using Eq. (3.5b) again, we find a quadratic equation for Z:

$$\tfrac{3}{4}Z^2-p\sqrt{2}Z+1=0. \tag{3.9}$$

In order that Eqs. (3.7) and (3.5b) have a real solution for A_1 and A_2, one must have $Z\geqslant 2\sqrt{2}$. This requirement selects one root of Eq. (3.9), and then we find

$$A_1=\frac{1}{2}\left\{\left(\frac{2\sqrt{2}}{3}\left(p+\sqrt{p^2-\tfrac{3}{2}}+3\right)\right)^{1/2} +\left(\frac{2\sqrt{2}}{3}\left(p+\sqrt{p^2-\tfrac{3}{2}}-3\right)\right)^{1/2}\right\},$$

$$A_2=\frac{1}{2}\left\{\left(\frac{2\sqrt{2}}{3}\left(p+\sqrt{p^2-\tfrac{3}{2}}+3\right)\right)^{1/2} -\left(\frac{2\sqrt{2}}{3}\left(p+\sqrt{p^2-\tfrac{3}{2}}-3\right)\right)^{1/2}\right\},$$

$$a=\left(\frac{4}{3}\left(2\sqrt{p^2-\tfrac{3}{2}}-p\right)\right)^{1/2} \tag{3.10}$$

(we assumed $A_1>A_2$ for definiteness). Note that this (real) solution exists for $p\geqslant\frac{7}{4}$. This threshold value $(p_0)_{\rm var}=\frac{7}{4}$ is only 5% larger than the exact bifurcation value $(p_0)_{\rm exact}=\frac{5}{3}$, at which point the asymmetric soliton of Eqs. (2.1) comes into existence (see Sec. II).

The other special case of an analytic solution of system (3.3) is when one takes

$$|A_1|=|B_1|=|A_2|=|B_2|\equiv A,\quad a=b,$$

$$\mathrm{sgn}(A_1A_2)=\mu,\quad \mathrm{sgn}(B_1B_2)=\nu,$$

where μ and ν can take on the values ± 1 independently of each other, and at the same time one relates the control parameters by

$$p-\mu=q-\nu.$$

In this case, Eqs. (3.3) readily yield the solution

$$A^2=\frac{4\sqrt{2}}{3}\frac{(p-\mu)}{1+\beta},\quad a^2=\tfrac{4}{3}(p-\mu), \tag{3.11}$$

which is the variational analogue of the composite vector soliton (2.8).

Although, as was mentioned in Sec. II, a general analytical solution to the VNLS (2.4) is not known, it will turn out

very useful in the future analysis to consider also the reduction of the DCDP to the VNLS model. To this end, one should take

$$A_1=\mu A_2\equiv A, \quad B_1=\nu B_2\equiv B, \quad \mu,\nu=\pm 1, \quad (3.12)$$

and then Eqs. (3.3) will reduce to

$$\frac{a^2}{4}+(p-\mu)-\frac{A^2}{\sqrt{2}}-\beta\frac{B^2 a}{\sqrt{a^2+b^2}}=0, \quad (3.13a)$$

$$\frac{b^2}{4}+(q-\nu)-\frac{B^2}{\sqrt{2}}-\beta\frac{A^2 b}{\sqrt{a^2+b^2}}=0, \quad (3.13b)$$

$$\frac{a^2}{4}-(p-\mu)+\frac{A^2}{2\sqrt{2}}+\beta\frac{B^2 a^3}{(\sqrt{a^2+b^2})^3}=0, \quad (3.13c)$$

$$\frac{b^2}{4}-(q-\nu)+\frac{B^2}{2\sqrt{2}}+\beta\frac{A^2 b^3}{(\sqrt{a^2+b^2})^3}=0. \quad (3.13d)$$

Equations (3.13) coincide with the equations that the variational method would yield for the VNLS model in which p and q would be replaced by $(p-\mu)$ and $(q-\nu)$, respectively. These equations, like the exact VNLS model (2.4), cannot be solved analytically unless $p-\mu=q-\nu$, which yields the special case of the vector soliton with a 45° angle of polarization; cf. Eqs. (3.13). However, the form of the general vector soliton (u_0,v_0) of the VNLS has been established numerically, and so we will consider its variational approximation, given by Eqs. (3.13), to be known. Consequently, we then know the form of the class of solitons of the DCDP that satisfies the reduction (3.12). We will call such solitons ''core symmetric,'' and the solitons that do not satisfy this reduction, ''core asymmetric.'' These names are chosen to emphasize a particular kind of symmetry with respect to interchanging the cores that the corresponding solitons have or do not have. Namely, for the core-symmetric solitons, magnitudes of the parallel components in the two cores are the same. Note that the core-symmetric solitons of the DCDP are the analogues of both the symmetric and antisymmetric solitons of the NLDC, whereas the core-asymmetric solitons are the analogs of the asymmetric solitons of the NLDC.

Thus it is the core-asymmetric solitons of Eqs. (3.3) that will be the remaining subject of our studies. Such solutions, in general, cannot be found analytically, but they can be found numerically by the Newton-Raphson method. From the above, it is also clear that Eqs. (3.3), in general, may have more than one solution for any given p and q. So, in order to find all the solutions, at least in some specified region of $A_{1,2}$, $B_{1,2}$, a, and b, we will use the following procedure. First, we will start to search for solutions where any of these six variables lies between the values of 0.1 $(=X_{\min})$ and $\sqrt{7[\max(p,q)+1]}$ $(=X_{\max})$. These values have been rather arbitrarily chosen, but as it will be clear from what follows, our numerical procedure still allows one to find solutions, if they existed, with values of $A_{1,2}$, $B_{1,2}$, a, and b outside the interval $(X_{\min},X_{\max})$, although such solutions were actually never found.

We divided the interval $(X_{\min},X_{\max})$ into smaller subintervals and thus obtained a six-dimensional grid in the space of the unknowns $A_{1,2}$, $B_{1,2}$, a, and b. At each node of the grid, we calculated the sum of the squares of the left-hand sides of Eqs. (3.3). If that sum was less than a certain number, denoted here as D, then we took the corresponding node of the grid as an initial guess in the Newton-Raphson method and then searched for a (real) root near that node. In fact, the structure of the basins of attraction of the roots of a system of nonlinear algebraic equations can be quite complicated [see, e.g., [20]], and, in particular, even fractal. So, even a close proximity of an initial guess to one of the roots does not always guarantee convergence to that root. However, we chose the threshold D to be not too small (usually, we took $D=6$) and thus obtained many nodes as initial guesses. This gave us confidence that we have probably not missed any of the actual roots.

From the above exposition of our numerical procedure, it is clear that implementing it did require a considerable amount of computer time. Therefore, any technique for obtaining information about the solutions of Eqs. (3.3) by solving fewer than six algebraic equations should be regarded as a very significant simplification. In Sec. IV, we will describe in detail two such techniques and also present the results that were obtained by utilizing them.

IV. BOUNDARIES OF REGIONS OF EXISTENCE OF SOLUTIONS OF EQS. (3.3)

Equations (3.3) have two control parameters, p and q. Therefore, the first question that needs to be answered is as follows: In what region(s) of the (p,q) plane do the solutions exist? We will only consider solutions that have all four amplitudes, $A_{1,2}$ and $B_{1,2}$ nonzero, since in the case when, say, $B_1=B_2=0$, the solutions were found analytically in Sec. III. It will be convenient to consider three different cases, distinguished by the relative signs of the amplitudes: case (i) $A_1A_2>0$ and $B_1B_2>0$; case (ii) $A_1A_2>0$ and $B_1B_2<0$; and case (iii) $A_1A_2<0$ and $B_1B_2<0$. Note that the signs of $A_{1,2}$ relative to those of $B_{1,2}$ are unimportant.

Let us first find the boundaries of the regions of existence of the core-symmetric solitons that satisfy the reduction (3.12). In that case, the exact equations for the boundaries can be found in the same way as it was done for the VNLS (2.4) [16,17]. The result is a simple generalization of Eq. (2.6):

$$(q-\nu)_{cr}^{\pm}=\left(\frac{\sqrt{1+8\beta}-1}{2}\right)^{\pm 2}(p-\mu), \quad (4.1)$$

where μ and ν were defined in Eq. (3.12). These boundaries are plotted in Figs. 1 and 2. Note that along the rays $q-\nu=(q-\nu)_{cr}^{-}$ and $q-\nu=(q-\nu)_{cr}^{+}$, one has $A=0$ and $B=0$, respectively.

We now show that the variational method provides a very good approximation to Eq. (4.1). In Eqs. (3.13), set $B=0$ (but $b\neq 0$), and then A and a are given by Eq. (3.6). Denoting $(b/a)=r$, one finds from Eqs. (3.13b), (3.13d), and (3.6)

$$(q-\nu)_{cr}^{+}=\frac{1}{3}\left(\frac{4\sqrt{2}\beta r}{\sqrt{1+r^2}}-r^2\right)(p-\mu), \quad (4.2a)$$

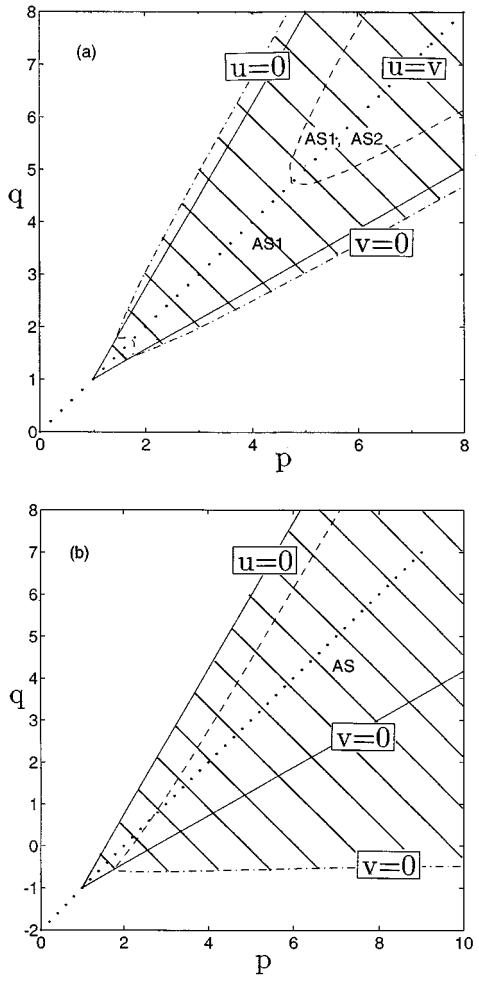

FIG. 1. Regions of existence of solutions of Eqs. (3.3) with $\beta=\frac{2}{3}$ in the (p,q) plane. (a) and (b) correspond to the cases ($A_1A_2>0$, $B_1B_2>0$) and ($A_1A_2>0$, $B_1B_2<0$), respectively; a figure for the case ($A_1A_2<0$, $B_1B_2<0$) is not shown. Note that in (b), $A_1=A_2$ and $B_1=-B_2$ along the bisector $p=q$ only for the core-symmetric soliton.

where r satisfies

$$\frac{r}{2}=\frac{\sqrt{2}\beta}{(\sqrt{1+r^2})^3}. \tag{4.2b}$$

Solving Eqs. (4.2) numerically for $\beta=\frac{2}{3}$ and $\beta=2$, one finds

$$\left[\frac{(q-\nu)^+_{cr}}{p-\mu}\right]_{\rm var}=2.426 \quad \text{versus} \quad \left[\frac{(q-\nu)^+_{cr}}{p-\mu}\right]_{\rm exact}=2.438 \quad \text{for } \beta=2 \tag{4.3a}$$

and

$$\left[\frac{(q-\nu)^+_{cr}}{p-\mu}\right]_{\rm var}=0.573 \quad \text{versus} \quad \left[\frac{(q-\nu)^+_{cr}}{p-\mu}\right]_{\rm exact}=0.575 \quad \text{for } \beta=\tfrac{2}{3}. \tag{4.3b}$$

Equations for the boundaries of regions of existence of core-asymmetric solitons of the DCDP cannot be found exactly, because even the exact form of the asymmetric solitons of the simpler NLDC model, Eq. (2.1), is not known. Therefore, we will use the variational approximation (3.10) for the asymmetric solitons of the NLDC to find the approximate boundaries of the regions of existence of the core-asymmetric solitons of the DCDP. Near such a boundary, one has that $B_{1,2}\ll A_{1,2}$ and $A_{1,2}$ are given, to the first order, by Eq. (3.10) (the case when $A_{1,2}\ll B_{1,2}$ can be treated analo-

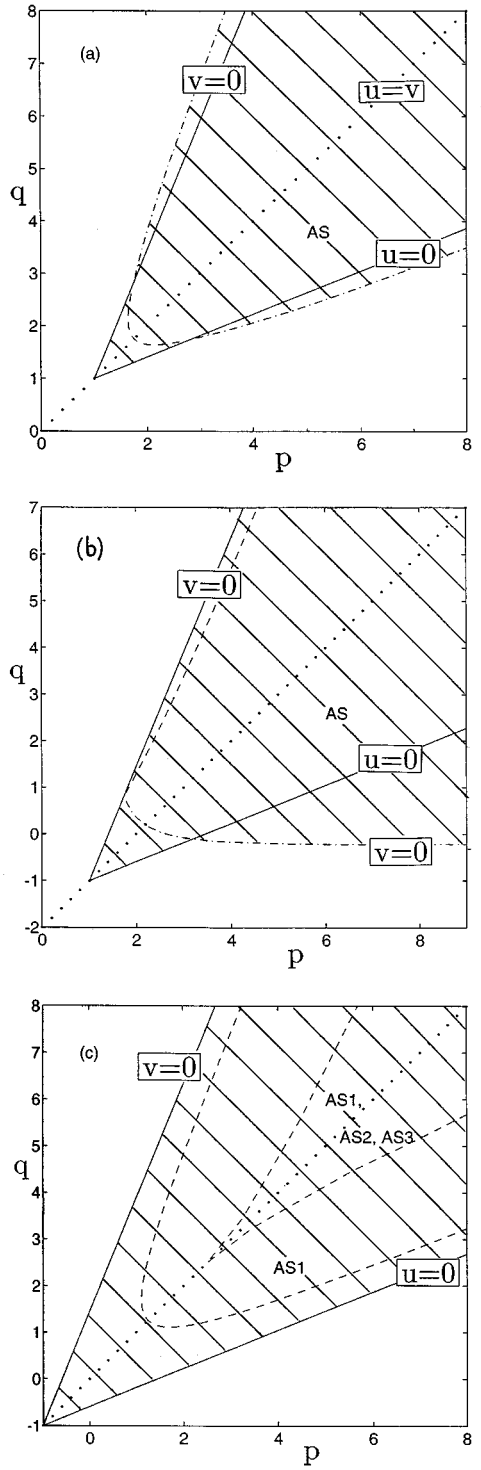

FIG. 2. Same as in Fig. 1, but $\beta=2$. Note that in (c), $A_1=-A_2$ and $B_1=-B_2$ along the bisector $p=q$ only for the core-symmetric and AS2 solitons.

gously). Note that A_1 and A_2 are of the same sign, while the infinitesimal amplitudes B_1 and B_2 could have opposite, as well as the same signs. Now, in Eqs. (3.3c) and (3.3d), one can neglect the terms proportional to B_1^2 and B_2^2 but one should keep the terms B_2/B_1 and B_1/B_2, respectively. Then, requiring that these equations be consistent with each other, i.e., that the ratio (B_2/B_1), found from Eq. (3.3c), be the inverse of the ratio (B_1/B_2), found from Eq. (3.3d), one obtains the equation

$$\left(\frac{b^2}{4}+q-\frac{\beta b A_1^2}{\sqrt{a^2+b^2}}\right)\left(\frac{b^2}{4}+q-\frac{\beta b A_2^2}{\sqrt{a^2+b^2}}\right)=1,$$

which, upon using Eqs. (3.5b) and (3.7), can be rewritten as

$$\left(\frac{b^2}{4}+q\right)^2-\left(\frac{b^2}{4}+q\right)\frac{\beta b Z}{\sqrt{a^2+b^2}}+\frac{2\beta^2 b^2}{a^2+b^2}=1. \quad (4.4)$$

Next, we substitute the values of (B_2/B_1) and (B_1/B_2), found from Eqs. (3.3c) and (3.3d), into Eq. (3.3f) in which we neglect the terms quadratic in $B_{1,2}$. This gives

$$\left(\frac{b^4}{16}-q^2\right)-\frac{1}{2}\left(\frac{b^2}{4}-q\right)\frac{\beta b Z}{\sqrt{a^2+b^2}}+\frac{\beta b^3}{2(\sqrt{a^2+b^2})^3}\times\left[Z\left(\frac{b^2}{4}+q\right)-\frac{4\beta b}{\sqrt{a^2+b^2}}\right]+1=0. \quad (4.5)$$

Equations (4.4) and (4.5), in which b and q are the unknowns and Z is the larger root of Eq. (3.9), determine the approximate boundaries of existence of the core-asymmetric solitons of the DCDP. Equations (4.4) and (4.5) were solved using the Maple symbolic calculations package, and the corresponding results are presented in Figs. 1 and 2 (dash-dotted lines). Naturally, it is much easier to solve (numerically) these two equations than the full set of six equations (3.3).

In reality, finding the boundaries of these regions still leaves the ambiguity as to on which side of the boundary the solution exists. A rigorous answer to this question requires carrying out more involved calculations than those presented above. Here we will only briefly describe the idea and the results, without going into details.

First, one lets

$$q=q_{cr}+\delta q,\quad a=a_{cr}+\delta a,\quad b=b_{cr}+\delta b,$$
$$A_{1,2}=(A_{1,2})_{cr}+\delta A_{1,2}$$

and

$$\delta a,\delta b,\delta A_{1,2},B_1^2,B_2^2=O(\delta q),$$

where the subscript cr denotes the value of the corresponding parameter at one of the boundaries (4.1). It is now convenient to denote $B_2/B_1=R$, with $R=O(1)$. Recall that the zeroth-order approximation R_{cr} is found from Eqs. (3.3c) and (3.3d), with the terms proportional to $B_{1,2}^2$ being neglected. When terms of order δq are retained, then $R=R_{cr}+\delta R$, and now Eqs. (3.3c) and (3.3d) are to be consistent with one another in the sense that $\delta(1/R)$, found from Eq. (3.3d), must be equal to $(-\delta R/R^2)$, where δR is found from Eq. (3.3c). Upon neglecting terms of order δq^2 and higher, this compatibility condition gives one *linear* equation for the five unknowns δa, δb, $\delta A_{1,2}$, and B_1^2 [since $B_2^2=B_1^2R_{cr}^2+O(\delta q^2)$]. The other four equations for these unknowns follow from Eqs. (3.3a), (3.3b), (3.3e), and (3.3f). By solving the resulting linear system, one finds that $B_1^2=K(p)\delta q$, where $K(p)$ is some coefficient. Then the requirement that $B_1^2>0$ selects on which side of the boundary the solution exists. For example, if $K(p)>0$, then the real solution exists for $\delta q>0$, and vice versa. The results that we found in this way are presented in Figs. 1 and 2 (the shaded areas denote the regions where the solutions exist), and these results are confirmed by the numerical solutions of Eqs. (3.3).

After we have determined the outer boundaries of the regions of existence of solutions, we determine the *bifurcation curves* inside those regions. At any given point of such a curve, a core-asymmetric soliton branches off from the core-symmetric soliton, similarly to what occurs for the NLDC solitons. Let us note that the following analysis can only determine the location of a *pitchfork* bifurcation, i.e., one for which the asymmetry between the components of the solution vanishes at the bifurcation point and increases gradually beyond it.

Thus, let us assume that the bifurcation occurs at $p=p_0$, $q=q_0$. Near the bifurcation point, i.e., for $p=p_0+\delta p$, $q=q_0+\delta q$, the asymmetry of the solution is small:

$$A_1=A_0+\delta A_1,\quad A_2=\mu(A_0+\delta A_2),\quad a=a_0+\delta a,$$
$$B_1=B_0+\delta B_1,\quad B_2=\nu(B_0+\delta B_2),\quad b=b_0+\delta b, \quad (4.6)$$

where A_0, B_0, a_0, and b_0 are the solutions of Eqs. (3.13), with the subindex 0 here and below denoting quantities that pertain to the bifurcation point. As is well known, at a pitchfork bifurcation, one has

$$\delta A_{1,2},\delta B_{1,2},\delta a,\delta b=O(\sqrt{\delta p},\sqrt{\delta q}).$$

Then, substituting Eq. (4.6) into Eq. (3.3) and retaining only the terms of order $(\sqrt{\delta p},\sqrt{\delta q})$, one obtains a *homogeneous linear* system for $\delta A_{1,2}$, $\delta B_{1,2}$, δa, and δb. After some rearrangement, that system separates into two systems: one is for $\Delta A\equiv\delta A_1-\delta A_2$ and $\Delta B\equiv\delta B_1-\delta B_2$, and the other for $\Sigma A\equiv\delta A_1+\delta A_2$, $\Sigma B\equiv\delta B_1+\delta B_2$, δa, and δb. One can show (the details are quite involved and therefore not given here) that the determinant of the latter homogeneous system is always nonzero for $\beta>0$, and thus that system has no nontrivial solutions. The condition under which a nontrivial solution ($\Delta A\neq 0$, $\Delta B\neq 0$) of the former system exists is

$$\left(\frac{\mu}{A_0^2}-\frac{1}{\sqrt{2}}\right)\left(\frac{\nu}{B_0^2}-\frac{1}{\sqrt{2}}\right)=\frac{\beta^2 a_0 b_0}{a_0^2+b_0^2}. \quad (4.7)$$

The existence of such a nontrivial solution is a manifestation of a *pitchfork* bifurcation occurring at the point (p_0,q_0), since for $\Delta A\neq 0$, $|A_1|$ is now slightly different from $|A_2|$. Thus for the control parameters p and q close to a bifurca-

tion point, along with the core-symmetric soliton, there is now a soliton with slight asymmetry between its components in the two cores, i.e., the core-asymmetric soliton.

To find the location of the bifurcation points, one first takes some (arbitrary) relation between $(p-\mu)$ and $(q-\nu)$, say,

$$(q-\nu)=\gamma(p-\mu), \tag{4.8}$$

and then inserts it into Eqs. (4.7) and (3.13), while considering $(p-\mu)$ as an unknown. Before we explain how this procedure was implemented for general γ in Eq. (4.8), let us observe that analytical solutions of Eqs. (3.13), (4.7), and (4.8) can be easily found in two particular cases. The first case is when, say, $B_0=0$, and then from Eq. (4.7) one has $A_0^2=\sqrt{2}$, which is equivalent to the bifurcation value for the asymmetric soliton of the NLDC; see Eq. (3.5b). The corresponding bifurcation points are found in Figs. 1 and 2 at the intersections of the dashed lines and the boundaries Eq. (4.1). The second special case is when $(p_0-\mu)=(q_0-\nu)$, $A_0=B_0$, and $a_0=b_0$; then A_0 and a_0 are found from Eq. (3.11), and Eq. (4.7) yields the following information.

(i) $\mu=1$, $\nu=1$ $(A_1A_2>0,\ B_1B_2>0)$: for $\beta>1$,

$$A_0^2=\frac{\sqrt{2}}{1+\beta},\quad p_0=\tfrac{7}{4}; \tag{4.9a}$$

for $\beta<1$,

$$(A_0^2)^{(1)}=\frac{\sqrt{2}}{1+\beta},\quad p_0=\tfrac{7}{4},$$

$$(A_0^2)^{(2)}=\frac{\sqrt{2}}{1-\beta},\quad p_0=1+\frac{3}{4}\frac{1+\beta}{1-\beta}. \tag{4.9b}$$

(ii) $\mu=1$, $\nu=-1$, $(A_1A_2>0,\ B_1B_2<0)$: for $\beta>1$,

no bifurcation point on the ray $q+1=p-1$; (4.10a)

for $\beta<1$,

$$A_0^2=\left(\frac{2}{1-\beta^2}\right)^{1/2}\quad p_0=1+\frac{3}{4}\left(\frac{1+\beta}{1-\beta}\right)^{1/2}. \tag{4.10b}$$

(iii) $\mu=-1$, $\nu=-1$ $(A_1A_2<0,\ B_1B_2<0)$: for $\beta>1$,

$$A_0^2=\frac{\sqrt{2}}{\beta-1},\quad p_0=-1+\frac{3}{4}\frac{1+\beta}{\beta-1}; \tag{4.11a}$$

for $\beta<1$,

no bifurcation point on the ray $q+1=p+1$. (4.11b)

These bifurcation points are found in Figs. 1 and 2 at the intersections of the bisector $(p-\mu)=(q-\nu)$ with the dashed lines. The knowledge of the location of the bifurcation points on the bisector as well as on the boundaries Eq. (4.1), already gives one a very good idea of what the bifurcation curves will be.

To solve the five equations (4.7) and (3.13) numerically when $(p-\mu)\neq(q-\nu)$, one proceeds as follows. Equations (3.13a) and (3.13b) can be viewed as a linear system for A^2 and B^2, and so can Eqs. (3.13c) and (3.13d). Then, requiring that A^2, found from Eqs. (3.13a) and (3.13b), be the same as A^2, found from (3.13c) and (3.13d), and similarly for B^2, one obtains the two equations

$$\left(\frac{1}{8}-\frac{\beta^2a^3b^3}{(a^2+b^2)^3}\right)\left(\frac{a^2}{4\sqrt{2}}+\frac{(p-\mu)}{\sqrt{2}}-\frac{\beta a}{\sqrt{a^2+b^2}}\times\left[\frac{b^2}{4}+(q-\nu)\right]\right)$$
$$=\left(\frac{1}{2}-\frac{\beta^2ab}{a^2+b^2}\right)\times\left(\frac{(p-\mu)}{2\sqrt{2}}-\frac{a^2}{8\sqrt{2}}-\frac{\beta a^3}{(\sqrt{a^2+b^2})^3}\left[(q-\nu)-\frac{b^2}{4}\right]\right), \tag{4.12a}$$

$$\left(\frac{1}{8}-\frac{\beta^2a^3b^3}{(a^2+b^2)^3}\right)\left(\frac{b^2}{4\sqrt{2}}+\frac{(q-\nu)}{\sqrt{2}}-\frac{\beta b}{\sqrt{a^2+b^2}}\times\left[\frac{a^2}{4}+(p-\mu)\right]\right)$$
$$=\left(\frac{1}{2}-\frac{\beta^2ab}{a^2+b^2}\right)\left(\frac{(q-\nu)}{2\sqrt{2}}-\frac{b^2}{8\sqrt{2}}-\frac{\beta b^3}{(\sqrt{a^2+b^2})^3}\times\left[(p-\mu)-\frac{a^2}{4}\right]\right). \tag{4.12b}$$

Taking into account Eq. (4.8), one observes from Eqs. (4.12) that a^2 and b^2 are proportional to $(p-\mu)$. Thus we can take

$$a=\tilde{a}\sqrt{p-\mu},\quad b=\tilde{b}\sqrt{p-\mu}, \tag{4.13}$$

which defines $\tilde{a}$ and $\tilde{b}$. Then, dividing Eqs. (4.12) through by $(p-\mu)$, one obtains two equations for $\tilde{a}$ and $\tilde{b}$, in which the parameter γ, defined in Eq. (4.8), plays the role of the control parameter. Solving those equations numerically with MAPLE, one finds $\tilde{a}$ and $\tilde{b}$ and then A^2 and B^2 from, say, Eqs. (3.13a) and (3.13b) as

$$A^2=\frac{(p-\mu)}{2}\left(\frac{\tilde{a}^2+4}{\sqrt{2}}-\frac{\beta\tilde{a}}{\sqrt{\tilde{a}^2+\tilde{b}^2}}[\tilde{b}^2+4\gamma]\right)\Bigg/\left(1-\frac{2\beta^2\tilde{a}\tilde{b}}{\tilde{a}^2+\tilde{b}^2}\right)\equiv K_A(\gamma)(p-\mu),$$

$$B^2=\frac{(p-\mu)}{2}\left(\frac{\tilde{b}^2+4\gamma}{\sqrt{2}}-\frac{\beta\tilde{b}}{\sqrt{\tilde{a}^2+\tilde{b}^2}}[\tilde{a}^2+4]\right)\Bigg/\left(1-\frac{2\beta^2\tilde{a}\tilde{b}}{\tilde{a}^2+\tilde{b}^2}\right)\equiv K_B(\gamma)(p-\mu). \tag{4.14}$$

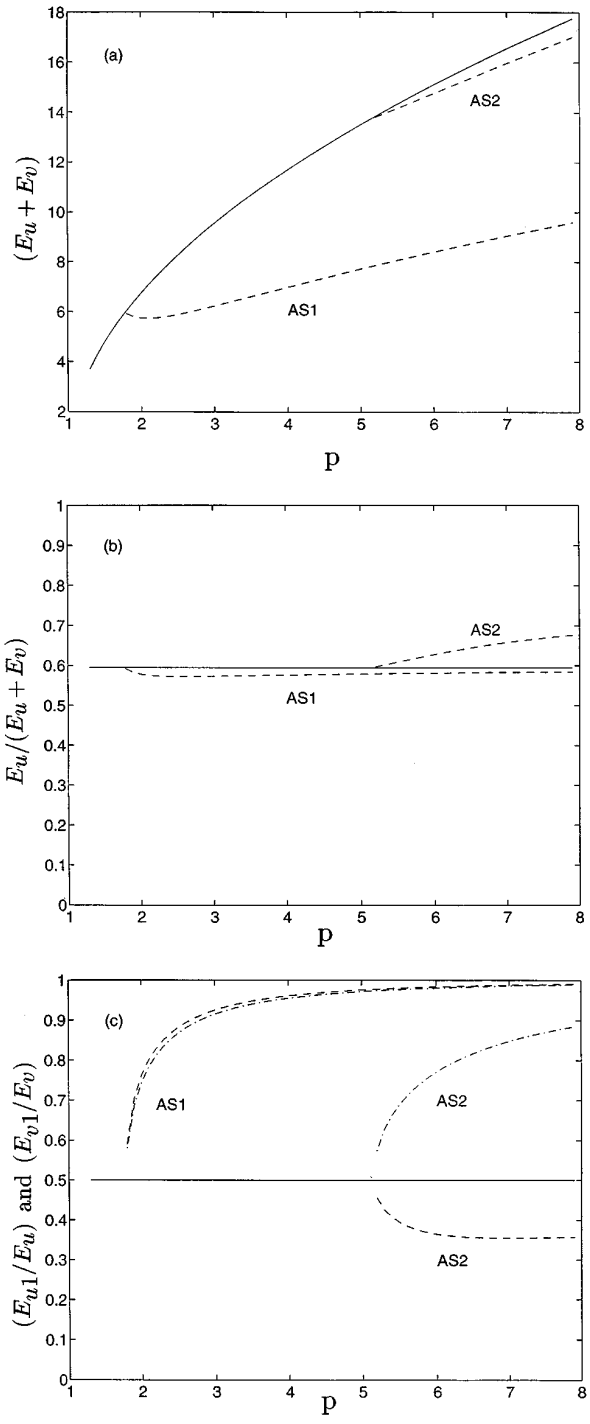

FIG. 3. (a) Total energy, $E=E_u+E_v$, of the soliton; (b) ratio of the energy in the u components to the total energy, E_u/E; (c) ratios E_{u1}/E_u and E_{v1}/E_v versus p for the case $\beta=\frac{2}{3}$, $A_1A_2>0$, and $B_1B_2>0$, $(q-1)=\gamma(p-1)$, where $\gamma=0.9$. The solid lines in all the three figures and the dashed lines in (a) and (b) show the results for the core-symmetric soliton and the core-asymmetric solitons, respectively. In (c), the dashed line shows (E_{u1}/E_u) and the dash-dotted line shows (E_{v1}/E_v) for the core-asymmetric solitons.

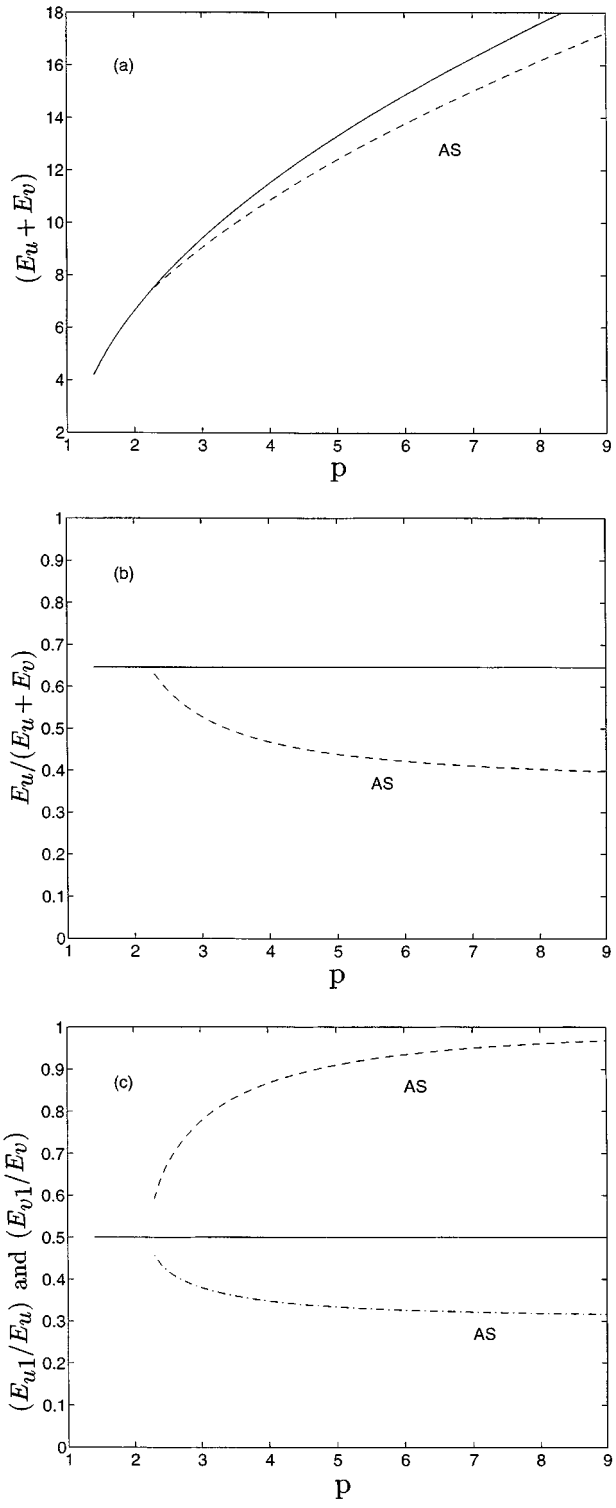

FIG. 4. Same as in Fig. 3, but now $(q-1)=\gamma(p-1)$ with $\gamma=0.85$ and $A_1A_2>0$, $B_1B_2<0$.

Substituting Eqs. (4.14) into Eq. (4.7) and solving the resulting quadratic equation for $(p-\mu)$, we obtain the location of the bifurcation point on the (p,q) plane as a function of the parameter γ. [Note that one should only keep the root(s) that yield(s) $A^2>0$ and $B^2>0$ according to Eqs. (4.14).] The results of such calculations are presented in Figs. 1 and 2 as the dashed lines [except for the second bifurcation curve in Fig. 2(c); see below].

Let us now explain why solving the equations for $\tilde{a}$ and $\tilde{b}$ with MAPLE is relatively easy, while solving the full system (3.3) with MAPLE would be very difficult. MAPLE's numerical solver requires an initial guess to be provided in order to find a root of a system of algebraic equations. Now,

when solving the equations for $\widetilde{a}$ and $\widetilde{b}$, we know the solution along the bisector $(p-\mu)=(q-\nu)$ and at the boundaries (4.1) [see the remark after Eqs. (4.11)], and hence we know how many solutions (zero, one, or two) we should expect. This limits the number of the initial guesses that one must make. On the contrary, when solving Eqs. (3.3) we do not know *for certain* how many solutions there will be. Even though the boundaries of the regions of existence and the bifurcation curves give the *minimum* number of solutions (for given p and q), there may exist other bifurcation curves that correspond to bifurcations other than pitchfork ones and which, therefore, cannot be found by the procedure described above. Such a bifurcation curve was indeed found (see Sec. V). Thus the *maximum* number of solutions to Eqs. (3.3) and, consequently, the number of the initial guesses one should take, is not known. Thus we found it essential to implement the scanning procedure described at the end of Sec. III.

V. NUMERICAL SOLUTION OF EQS. (3.3)

In this section, we will present the plots of the regions of existence of various types of the soliton solutions of Eqs. (1.1), as given by their variational approximations, Eqs. (3.3), and describe what a representative soliton of each type looks like. In Figs. 1 and 2 we have plotted the regions of existence of the solutions in the (p,q) plane (shaded areas). The boundaries of those regions were obtained as explained in Sec. IV, and in all the cases but one [see Fig. 2(c)], no other boundaries were found from the numerical solution of the full system (3.3). This justifies the effort made on the analysis that we did in Sec. IV.

The general comments about all the plots in Figs. 1 and 2 are as follows. First of all, we recall that outside the shaded areas, there exists only solutions with either both u or both v components vanishing (cf. Sec. III). Next, inside the open angles bounded by the straight lines, there are always the core-symmetric solitons satisfying condition (3.12). The asymmetric solitons exist inside the upper right-hand part of the bifurcation curves (dashed lines), except for the case depicted in Fig. 2(b); see below. The dash-dotted lines in these two figures represent the boundaries where two of the components (either $u_{1,2}$ or $v_{1,2}$) must vanish and the resulting two-component soliton coincides with the asymmetric soliton of the NLDC.

In Figs. 3–7, we plotted the dependences of the energy of the soliton's components, where the energies are defined by the formulas

$$E_{u1}=\int_{-\infty}^{\infty}|u_1|^2 d\tau, \quad E_{u2}=\int_{-\infty}^{\infty}|u_2|^2 d\tau, \quad E_u=E_{u_1}+E_{u_2},$$

$$E_{v1}=\int_{-\infty}^{\infty}|v_1|^2 d\tau, \quad E_{v2}=\int_{-\infty}^{\infty}|v_2|^2 d\tau, \quad E_v=E_{v_1}+E_{v_2}, \tag{5.1}$$

versus p [in what follows to be called ''$(E-p)$ diagrams''], with q changing along the rays (4.8) for some representative values of γ. (Note that for any one core-asymmetric soliton, there is actually a pair of such solutions, with one member of the pair differing from the other by interchanging the subscripts 1 and 2.)

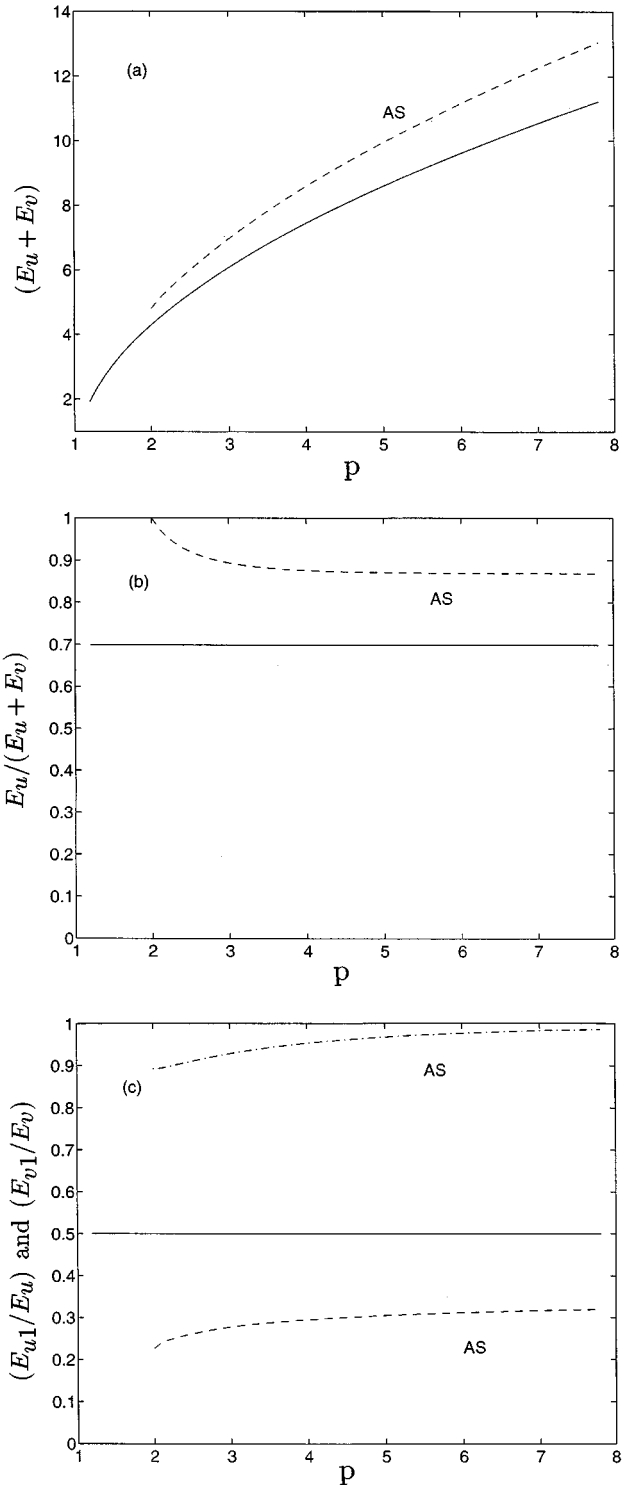

FIG. 5. Same as in Fig. 4, but $\beta=2$ and $\gamma=1.4$.

Now we give specific comments about the plots in Figs. 1–7.

In Figs. 1(a) and 3, $\beta=\frac{2}{3}$, $A_1A_2>0$, and $B_1B_2>0$. For sufficiently large p and q, one has a second pair of core-asymmetric solitons [labeled ''AS2'' in Fig. 1(a)], which are created as a result of a pitchfork bifurcation from the core-symmetric soliton. Thus the total number of solutions changes, as one crosses the bifurcation curves from left to right, from 1 to 3 and then to 5. One can see, from Fig. 3,

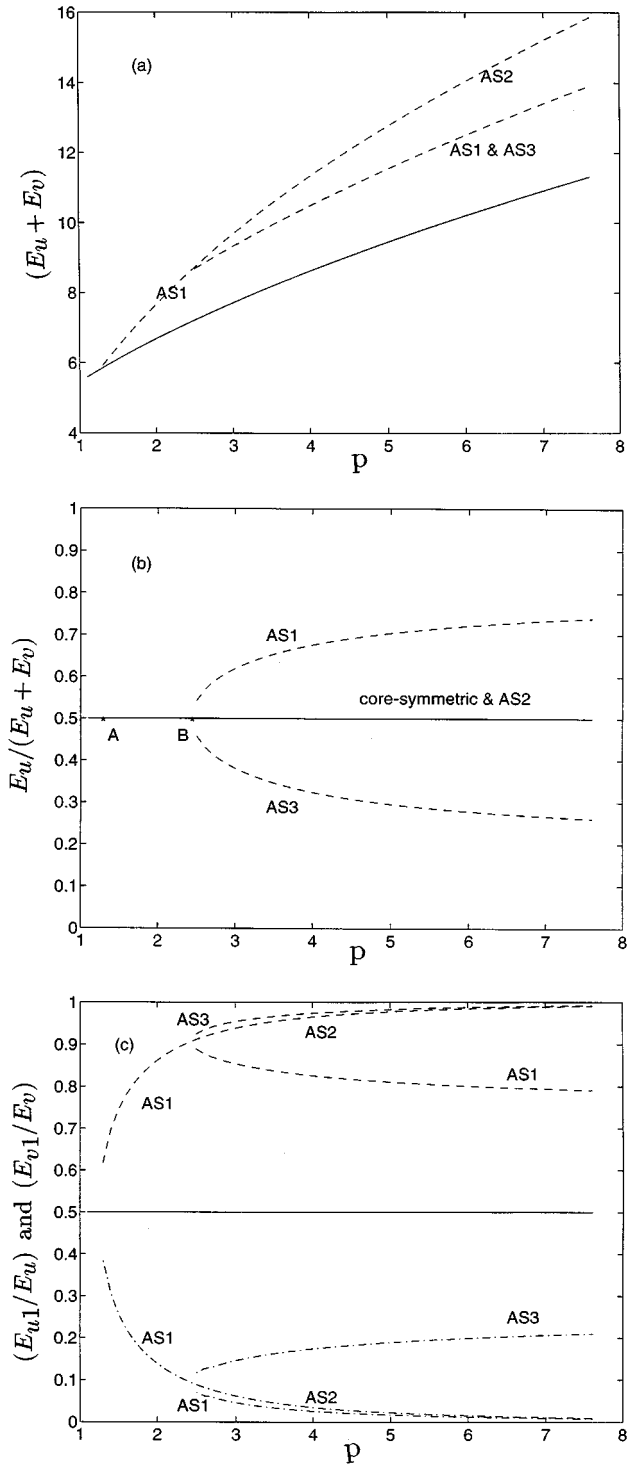

FIG. 6. Same as in Fig. 5, but $A_1A_2<0$, $B_1B_2<0$, and $(q+1)=\gamma(p+1)$ with $\gamma=1$. Note also that in (b), the solid line between points A and B represents the behavior of both the core-symmetric and AS1 solitons, whereas on the right of point B, it represents the behavior of the core-symmetric and AS2 solitons.

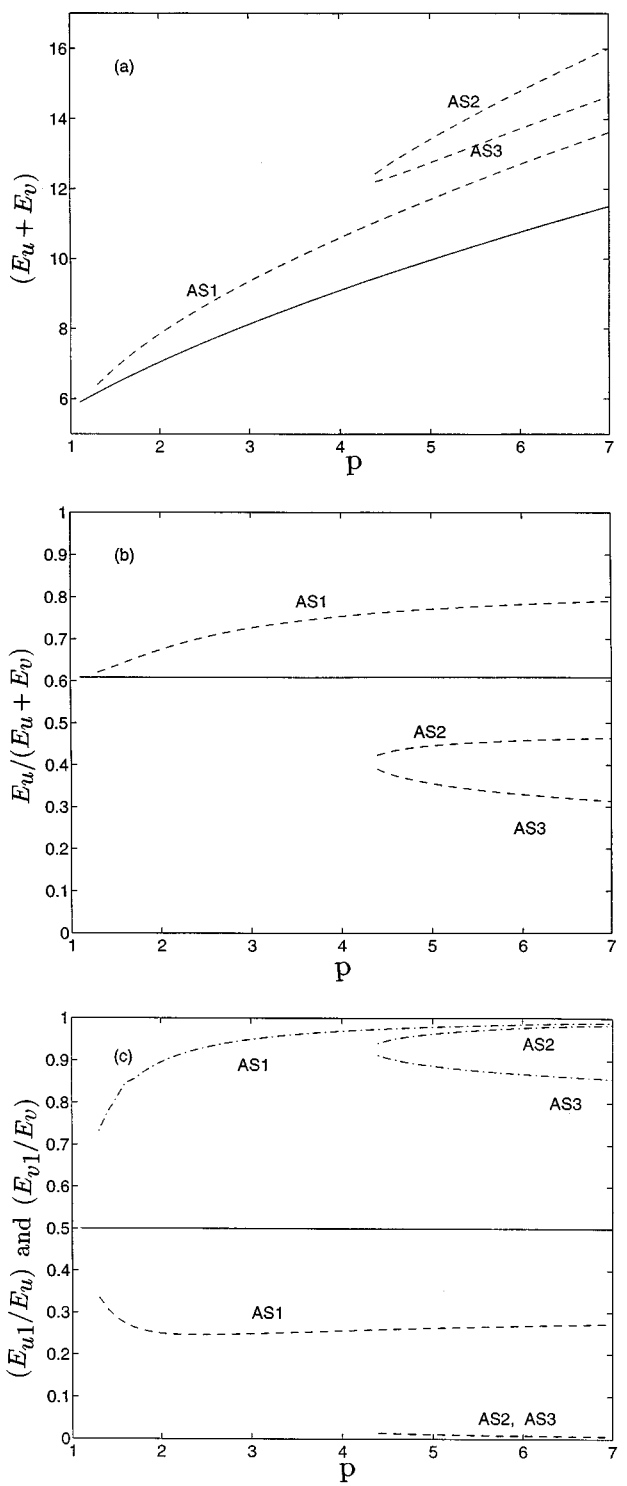

FIG. 7. Same as in Fig. 6, but $\gamma=1.2$.

that for the first core-symmetric soliton [labeled ''AS1'' in Fig. 1(a)],

$$(u_1,v_1)\rightarrow(u_0,v_0),\quad (u_2,v_2)\rightarrow(0,0) \tag{5.2a}$$

as $p,q\rightarrow\infty$, where (u_0,v_0) is the vector soliton of the VNLS (2.4) for the given p and q. (By convention, we consider u_0 and v_0 to be positive.) The following remarks need to be made about formula (5.2a) and similar formulas in the remainder of this section. It can be shown (see Appendix A) that the limit ($p,q\gg1$, κ fixed) taken in Eqs. (1.1) is equivalent to the limit (p,q fixed, $\kappa\ll1$). Therefore, for large p and q, the solitons in the two cores can be considered as only weakly coupled to each other. Therefore, in this limit, the form of the soliton in either core must asymptotically tend to that of one of the possible solutions of the VNLS (2.4). The

role of the variational method is that it determines which particular configuration of the soliton components is realized in each concrete case.

Now, the second core-asymmetric soliton has, in the same limit $p,q\to\infty$ and for $\gamma<1$,

$$(u_1,v_1)\to(u_0,v_0),\quad (u_2,v_2)\to(u_{00},0), \tag{5.2b}$$

where u_{00} and v_{00} were defined in Eq. (2.7). (For $\gamma>1$ the situation is reversed by interchanging u and v.) The form of the core-symmetric soliton with a given value of γ is the same as the form of the vector soliton of the VNLS with $(q/p)=\gamma$. Equations (5.2), and their analogs for other cases below, allow one to extrapolate the $(E-p)$ diagrams, found for a specific value of γ, to other values of γ.

It is worth noting that the first core-asymmetric soliton above is a four-component analog of the asymmetric soliton of the NLDC, since for it

$$\frac{A_1}{A_2}\approx\frac{B_1}{B_2}. \tag{5.3}$$

The asymptotic behavior, expressed by Eq. (5.2b), of the AS2 soliton also deserves a separate remark. Indeed, Eq. (5.2b) holds for the case $\gamma<1$, whereas for $\gamma>1$, as noted above, the u and v components of the soliton must be interchanged. Thus the asymptotic form of the AS2 soliton for $\gamma>1$ is

$$(u_1,v_1)\to(u_0,v_0),\quad (u_2,v_2)\to(0,v_{00}). \tag{5.2c}$$

Comparing Eq. (5.2b) with Eq. (5.2c), one sees that there is a discontinuity in the soliton's form when γ crosses the value of 1. Of course, in reality, the solution of Eqs. (3.3) must be continuous with respect to the control parameters p and q (and, consequently, γ). The key to resolving this seeming contradiction lies in keeping the correct order when passing to the limits $(p,q)\to\infty$ and $\gamma\to1$. We present the details of the explanation in Appendix B; here we will only note that in all the other five cases considered below, such a situation does not occur.

In Figs. 1(b) and 4, $\beta=\frac{2}{3}$, $A_1A_2>0$, and $B_1B_2<0$. For both $\gamma<1$ and $\gamma>1$, the asymptotic (as $p,q\to\infty$) form of the core-asymmetric soliton is

$$(u_1,v_1)\to(u_0,v_0),\quad (u_2,v_2)\to(0,-v_{00}). \tag{5.4}$$

We did not present a separate figure for the case $\beta=\frac{2}{3}$, $A_1A_2<0$, and $B_1B_2<0$ since only the core-symmetric solitons exist in this case. The domain of existence of those solutions is the open angle bounded by the straight lines whose equations are given by Eq. (4.1) with $\nu=\mu=-1$.

In Fig. 2(a), $\beta=2$, $A_1A_2>0$, and $B_1B_2>0$. We did not present the $(E-p)$ diagram for the core-asymmetric soliton in this case because it (the diagram) is very similar to that for the first core-asymmetric soliton in Fig. 3. The only difference between those two cases is that for the core-asymmetric soliton in the present case, the ratio (v_2/v_1) tends to zero a little bit faster than the ratio (u_2/u_1) does as $p,q\to\infty$, while in Fig. 3, the situation was the opposite. Thus the core-asymmetric soliton in this case is also a four-component analogue of the asymmetric soliton of the NLDC.

In Figs. 2(b) and 5, $\beta=2$, $A_1A_2>0$, and $B_1B_2<0$. Between the upper straight line boundary and the dashed curve corresponding to a pitchfork bifurcation, there exists a core-asymmetric soliton with very small v components. Moreover, a feature that is not seen in this figure, because of the latter's limited scope, but that can be found from Eqs. (4.7) and (4.12)–(4.14), is that the bifurcation curve comes closer to the straight line boundary as p and q increase, and so for p and q large enough, the v components of that core-asymmetric soliton approach zero. For this reason, we chose not to present a separate $(E-p)$ diagram for that solution.

Next, let us emphasize that the dash-dotted curve, even though it passes through the interior of the open angle, is *not* a curve of a pitchfork bifurcation occuring from the core-symmetric soliton. In fact, the core-asymmetric soliton along that part of the curve is *distinctly* different from the core-symmetric soliton existing for the same values of p and q (except at the point $[p=\frac{7}{4},\ q=q_{cr}^{+}(\frac{7}{4})]$).

Note that for both $\gamma<1$ and $\gamma>1$, the asymptotical form of the core-asymmetric soliton is

$$(u_1,v_1)\to(u_0,v_0),\quad (u_2,v_2)\to(u_{00},0). \tag{5.5}$$

In Figs. 2(c), 6, and 7, $\beta=2$, $A_1A_2<0$, and $B_1B_2<0$. The second bifurcation curve (the one with the cusp) corresponds to the occurrence of *two* pairs of core-asymmetric solitons that branch off from the already existing core-asymmetric soliton as a result of a *saddle-node* bifurcation. This second bifurcation curve, which could not be found by the methods described in Sec. IV, was found numerically by solving all six Eqs. (3.3). The number of solutions in this case changes, as one crosses the bifurcation curves from left to right, from 1 to 3 and then to 7. We will denote the three different types of the core-asymmetric solitons as AS1, AS2, and AS3. The trends in their $(E-p)$ diagrams are clearly seen from Figs. 6 and 7, which correspond to $\gamma=1$ and $\gamma=1.2$, respectively. Note the nonsmooth behavior of the curves corresponding to the AS1 soliton in Fig. 6: such a behavior is characteristic of a *degenerate* (due to $\gamma=1$) saddle-node bifurcation, which occurs to that soliton. Note also that the corresponding curves in Fig. 7 become smooth, since the degeneracy of the saddle-node bifurcation is now removed. For $\gamma>1$ we have

$$(u_1,v_1)\to(u_0,v_0),\quad (u_2,v_2)\to(-u_{00},0)\quad \text{for AS1}, \tag{5.6a}$$

$$(u_1,v_1)\to(0,v_{00}),\quad (u_2,v_2)\to(-u_{00},0)\quad \text{for AS2}, \tag{5.6b}$$

$$(u_1v_1)\to(0,v_{00}),\quad (u_2,v_2)\to(-u_0,-v_0)\quad \text{for AS3} \tag{5.6c}$$

as $p,q\to\infty$.

VI. CONCLUSIONS

In this work, we have addressed the problem of the existence of various types of solitons of the DCDP (1.1). These equations are a generalization of the NLDC model (2.1) for the case when polarization of light is taken into account. Therefore, it was natural to draw analogies with the known results for the NLDC and also with the single core with two

orthogonal polarizations, described by the VNLS (2.4).

To find the various types of solitons of the DCDP, we employed the variational method, in which we approximated the exact profiles of the solitons by Gaussians. In that way, we found that there are several types of solitons that can be classified as follows: (i) core-symmetric solitons that are the analogs of the symmetric and antisymmetric solitons of the NLDC, (ii) core-asymmetric solitons that for large values of their energy have almost all the energy concentrated in one of the cores, and (iii) core-asymmetric solitons for which the ratio of the energies in the two cores is finite in the limit of infinite total energy. Group (ii) includes, for $\beta=\frac{2}{3}$, the AS1 soliton in Fig. 1(a), and for $\beta=2$, it includes the core-asymmetric soliton in Fig. 2(a) and the core-asymmetric soliton with small v components in Fig. 2(b). Group (iii) includes all the other types of the core-asymmetric solitons. All of the core-asymmetric solitons exist only above certain threshold values of the soliton's energy. In most cases, we were able to determine the corresponding bifurcation curves without solving the full system of the variational equations, Eqs. (3.3). On the contrary, the core-symmetric solitons can exist for any value of the energy, with equal energy propagating in each core.

Let us note the following about the solitons of group (iii) whose regions of existence are shown in Figs. 1(b) and 2(b). Parts of these regions are located below the line $q=1$. For $-1<q<1$ and $p>1$, the *linearized* Eqs. (1.1), in which the z dependence is replaced by factors e^{ipz} and e^{iqz} according to Eq. (3.1), have both exponential and oscillatory solutions. It is known that the presence of the latter implies that the stationary solutions of the full, nonlinear Eqs. (1.1) may be not exponentially localized but instead may have oscillating ''tails'' with asymptotically constant amplitude. An example of such a situation can be found in [19]. Therefore, it is possible that the core-asymmetric solitons of Eqs. (1.1) for $-1<q<1$ also have oscillating tails, even though the variational method, being based on the Gaussian ansatz, yields a localized solution in that region. Determining whether or not this is actually the case would require numerically solving the corresponding ordinary differential equation reduction of Eqs. (1.1), which we do not attempt here. Note that the core-symmetric solitons must be exponentially localized even for $-1<q<1$, because for these, the effective value of the propagation constant of the v component is $(q+1)>0$ rather than just q; cf. Eq. (3.13).

Now we will briefly comment on the stability of the various types of solitons in the limit of large total energies, $E=E_u+E_v\to\infty$. In Sec. V, the variational method allowed us to determine the exact asymptotic form of the solitons in this limit. For sufficiently large but still finite values of E, the solitons take on their respective forms, Eqs. (5.2), (5.4)–(5.6) *plus* some small corrections, whose magnitude is of the order $1/E$ and which, in principle, can be computed. The stability results reported below pertain to these, asymptotically exact, solitons. The details of our stability analysis will be presented elsewhere [15]. All but one type of solitons in group (i), and all but one type of solitons in group (iii), are unstable when $E\gg 1$, with the instability growth rate λ being on the order of $O(E)=O(\sqrt{p},\sqrt{q})$. Note that in the soliton's own reference frame, this instability is weak, since a typical distance (''soliton period'') over which the soliton can undergo significant changes is scaled as $p^{-1}=O(E^{-2})$. Thus a sufficiently high-energy (and hence narrow), unstable soliton can still propagate several $[<O(E)]$ soliton periods along the fiber before being significantly changed by the instability. The exceptional solitons of group (iii), denoted as AS2 in Fig. 2(c) have an instability growth rate of $\lambda=O(1)$, which is much slower than that of the other unstable solitons. Thus such a soliton could exist for many $[<O(E^2)]$ soliton periods, and so it could possibly be observed, as a transient state, in a numerical or a real-world experiment with the DCDP model. Let us note that in [14], it was reported that certain unstable solitons (called there ''*A*-type states'') could also propagate in low-birefringence fibers over relatively long distances before decaying.

As for the exceptional case of solitons of group (i), which is the core-symmetric soliton in Fig. 2(a), its stability or instability could not be established within the framework of the first-order calculations carried out in [15]. One could only state that the instability growth rate, if any, for such solitons would be on the order of 1 *at the largest* (in the limit $E\gg 1$). In fact, if further studies would reveal that $\lambda=o(1)$, then that would mean that this type of circularly polarized, core-symmetric soliton is quasistable (or stable, if $\lambda=0$) for large energies. This would be in distinct contrast with the NLDC, where the symmetric solitons have an instability growth rate $\lambda=O(E)$ for $E\gg 1$. We also remark that in analogy with the results for the NLDC, all types of the core-symmetric solitons of the DCDP are likely to be stable for sufficiently low value of their energy.

The two types of solitons of group (ii) whose regions of existence in the (E_u,E_v) plane are shown in Figs. 1(a) and 2(a), have been proven in [15] to be stable for large values of their energy. Using the analogy with the asymmetric soliton of the NLDC, we speculate that these two types of solitons of Eqs. (1.1) are also stable over most of the region of their existence. Let us note that if future studies reveal that the core-symmetric soliton in Fig. 2(a) is either stable or quasistable, as explained above, then one would have (quasi)bistability between the core-symmetric and core-asymmetric solitons in the DCDP circular polarizations. For the third type of solitons of group (ii), the stability analysis in the limit $E\gg 1$ is trivial, because in this limit the soliton becomes almost identical with the two-component asymmetric soliton of the NLDC, and thus it must be stable. Since the solitons of this type have rather small v components [see Fig. 2(b)] and hence are close to the two-component asymmetric solitons for any value of their energy, then we speculate that such solitons must be stable for almost all values of their energy.

APPENDIX A: SCALING TRANSFORMATION FOR EQS. (1.1) AND (3.3)

Here we will show that the limit $(p,q)\to\infty$ in Eqs. (3.3) is equivalent to the limit of weak coupling of the two cores. To this end, we first notice that solitons of Eqs. (3.3) [and Eqs. (1.1)] with $p,q\gg 1$ have large amplitudes and small widths, which is seen from the special solutions presented in Secs. II and III and also was confirmed by our numerical solution of Eqs. (3.3). Next, one can perform the following scaling transformation in Eqs. (1.1):

$$u=\tilde{u}/\sqrt{\varepsilon},\quad v=\tilde{v}/\sqrt{\varepsilon},\quad \tau=\tilde{\tau}\sqrt{\varepsilon},\quad z=\tilde{z}\varepsilon. \tag{A1}$$

Let the amplitudes $\tilde{u}$ and $\tilde{v}$, as well as the soliton's width and dispersion length expressed in terms of the rescaled coordinates $\tilde{\tau}$ and $\tilde{z}$, respectively, have their magnitudes of order 1. Then taking the limit $\varepsilon \ll 1$ in Eq. (A1) corresponds to the limit $p,q \gg 1$ in terms of the original variables. [In fact, the propagation constants are rescaled as follows: $p=\tilde{p}/\varepsilon$ and $q=\tilde{q}/\varepsilon$, where $\tilde{p},\tilde{q}=O(1)$.] On the other hand, the tilded quantities satisfy Eqs. (1.1) with $\tilde{\kappa}=\varepsilon$ [recall that we set $\kappa=1$ in Eqs. (1.1)]. Thus we have shown that the limit ($p,q \gg 1$, κ fixed) in Eqs. (1.1) is equivalent to the limit (p,q fixed, $\kappa \ll 1$), which is the limit of small coupling between the cores.

APPENDIX B: ASYMPTOTIC BEHAVIOR OF THE SECOND CORE-ASYMMETRIC SOLITON IN FIG. 1(a)

Here we will show how the seeming contradiction, indicated in the main text, regarding the asymptotic form of the AS2 soliton in Fig. 1(a) is resolved. First, we notice that when $\gamma=1$, then that soliton has the following symmetry of its components:

$$u_1=v_2, \quad u_2=v_1, \quad u_1 \neq u_2. \tag{B1}$$

The existence of this solution was confirmed by explicit numerical solution of Eqs. (3.3). Note that when $p=q \to \infty$, $u_2=O(\sqrt{p})$ and $u_1=O(1/\sqrt{p})$. (For definiteness, we will *not* consider here the equivalent case where the subscripts 1 and 2 are interchanged.) Thus the asymptotic form of that soliton is ($\gamma=1$)

$$(u_1,v_1) \to (0,v_{00}), \quad (u_2,v_2) \to (u_{00},0). \tag{B2}$$

Now, if one fixes p (or q) to be some large but finite value, while changing γ slightly so that $(\gamma-1)$ is sufficiently small, then the resulting solution, by continuity, must take the form

$$(u_1,v_1) \to [(\hat{O},v_{00}(1+\hat{O}))], \quad (u_2,v_2) \to [(u_{00}(1+\hat{O}),\hat{O})], \tag{B3}$$

where the notation $\hat{O}$ is used for a quantity that satisfies

$$\lim_{p \to \infty} \lim_{\gamma \to 1} \hat{O} = 0. \tag{B4}$$

Note that in Eq. (B4), the limit $\gamma \to 1$ must be taken first. The asymptotic form (B3) of the soliton in question is different from both Eqs. (5.2b) and (5.2c). However, if one now first fixes γ at some value not equal to 1 and *then* considers the limit of large p (and q), then the asymptotic form of the AS2 soliton in Fig. 1(a) will indeed be given by either Eqs. (5.2b) or (5.2c). We verified the validity of this statement by numerically solving Eqs. (3.3) for $\gamma=0.97$ ($\beta=\frac{2}{3}$, $A_1A_2>0$, and $B_1B_2>0$) and p between 5 and 50 (the corresponding plots are not presented here due to lack of space). We observed that, for the values of parameters specified in the previous sentence, the numerical solution agrees reasonably well with Eq. (B1) for $p<8$, whereas it begins to shift towards the asymptotic form Eq. (5.2b) for $p>15$. For $p \approx 50$, the difference between the numerical solution and the corresponding asymptotics Eq. (5.2b) is less than 10%. This suggests that the quantity $\hat{O}$ above must have the order of magnitude $O(\sqrt{\gamma-1})O(1/\sqrt{p})$. Thus we have demonstrated that there is no contradiction between the continuity of the solution of Eqs. (3.3) with respect to the control parameters, on one hand, and the asymptotic formula (5.2b) [or (5.2c)] for the AS2 soliton in Fig. 1(a), on the other.

[1] A. W. Snyder, D. J. Mitchell, L. Poladian, D. R. Rowland, and Y. Chen, J. Opt. Soc. Am. B **8**, 2102 (1991).

[2] M. Romangoli, S. Trillo, and S. Wabnitz, Opt. Quantum Electron. **24**, S1237 (1992).

[3] N. Akhmediev and A. A. Ankiewicz, Phys. Rev. Lett. **70**, 2395 (1993); P. L. Chu, B. A. Malomed, and G. D. Peng, J. Opt. Soc. Am. B **10**, 1379 (1993).

[4] J. M. Soto-Crespo and N. Akhmediev, Phys. Rev. E **48**, 4710 (1993).

[5] N. N. Akhmediev and A. V. Buryak, J. Opt. Soc. Am. B **11**, 804 (1994).

[6] S. L. Doty, J. W. Haus, Yun Je Oh, and R. L. Fork, Phys. Rev. E **51**, 709 (1995).

[7] I. M. Uzunov, R. Muschall, M. Gölles, Yu. S. Kivshar, B. A. Malomed, and F. Lederer, Phys. Rev. E **51**, 2527 (1995).

[8] B. A. Malomed, I. M. Skinner, P. L. Chu, and G. D. Peng, Phys. Rev. E **53**, 4084 (1996).

[9] M. N. Islam, *Ultrafast Fiber Switching Devices and Systems* (Cambridge University Press, Cambridge, 1992), Chap. 2.

[10] A. Hasegawa and Y. Kodama, *Solitons in Optical Communications* (Clarendon, Oxford, 1995).

[11] C. R. Menyuk, IEEE J. Quantum Electron. **QE-25**, 2674 (1989).

[12] C. R. Menyuk and P. K. A. Wai, J. Opt. Soc. Am. B **11**, 1305 (1994).

[13] J. Yang and D. J. Benney, Stud. Appl. Math. **96**, 111 (1996).

[14] N. N. Akhmediev, A. V. Buryak, J. M. Soto-Crespo, and D. R. Andersen, J. Opt. Soc. Am. B **12**, 434 (1995).

[15] T. Lakoba and D. Kaup (unpublished).

[16] V. M. Eleonsky *et al.*, Zh. Eksp. Teor. Fiz. **99**, 1113 (1991) [Sov. Phys. JETP **72**, 619 (1991)].

[17] M. Haelterman and A. P. Sheppard, Phys. Lett. A **194**, 191 (1994).

[18] D. Anderson, Phys. Rev. A **27**, 3135 (1983).

[19] D. J. Kaup, T. I. Lakoba, and B. I. Malomed, J. Opt. Soc. Am. B (to be published).

[20] I. Peterson, *The Mathematical Tourist* (Freeman, New York, 1988), Chap. 6, pp. 164–170.